Tracking, vertexing and b-tagging performance at ATLAS

Sara Strandberg, on behalf of the ATLAS Collaboration
Stockholm University
Department of Physics
106 91 Stockholm, Sweden

1 Introduction

The ATLAS experiment [1] is a general purpose experiment that records collision events produced by the Large Hadron Collider (LHC) [2] at CERN. Surrounding the interaction point, the experiment is equipped with an Inner Detector (ID) tracking system embedded in a 2 T axial magnetic field. The ID consists of two silicon-based detectors (a Pixel detector and a microstrip detector, SCT) closest to the interaction point surrounded by a transition radiation tracker (TRT). The electromagnetic and hadronic calorimeters are located outside the ID solenoid, and are both based on sampling techniques. Finally a muon detector system immersed in a toroidal magnetic field occupies the outermost region of the detector.

The LHC started its operations late 2009, and during 2010 and 2011 it has produced proton-proton collisions at 7 TeV. The integrated luminosity recorded by ATLAS amounts to approximately 40 pb^{-1} in 2010 and 5 fb^{-1} in 2011.

2 Track Reconstruction

Tracks are reconstructed within the full ID acceptance ($|\eta| < 2.5$) using a χ^2 fitter. The pattern recognition [3] works primarily inside-out, starting with a seed in the silicon-based detectors and extrapolating outwards to also include measurements in the TRT. To recover e.g. tracks from secondary interactions there is also an outside-in tracking, which uses TRT track segment seeds and extrapolates inwards. The track candidates are finally required to fulfill a set of quality criteria, based e.g. on the number of silicon hits and the transverse and longitudinal impact parameters with respect the beam spot.

The high instantaneous luminosity of the LHC leads to a large number of additional proton-proton collisions per event (pileup) and thus a relatively high occupancy in the ID. This in turn increases the rate of fake tracks reconstructed from random combinations of ID measurements. To limit the rate of fake tracks, a robust track reconstruction configuration has been developed which makes more stringent hit requirements [5]. Fig. 1 (left) shows the fraction of fake tracks in three pileup scenarios with the default and robust track reconstruction configuration.

To allow for a precise measurement of the track parameters, a track-based alignment of the ATLAS ID is carried out through a χ^2 minimization of the track-hit residuals. In addition, constraints from the invariant masses of e.g. K_s^0 mesons and Z bosons are used, as well as the ratio of the energy of electrons measured in the calorimeters and the corresponding momentum measured in the ID (E/p). Fig. 1 (middle) shows the difference between the reconstructed and true K_s^0 mass as a function of the azimuthal angle ϕ in 2010 and 2011, highlighting the much reduced bias of the track parameters achieved by an improved alignment of the ID in 2011. Fig. 1 (right) shows the data-to-simulation comparison of the transverse impact parameter, d_0, of tracks in the forward region. The resolution reaches the design value for low p_{T} tracks while it is slightly worse than predicted for high p_{T} tracks due to residual misalignments present in the data.

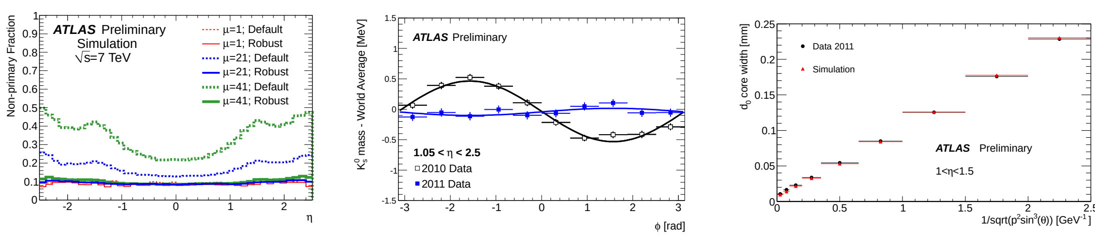

Figure 1: Left: The fraction of fake tracks in three pileup scenarios for the default and robust track reconstruction configuration [5]. Middle: The difference between the reconstructed and true K_s^0 mass as a function of the azimuthal angle ϕ in 2010 and 2011 [6]. Right: The width of the core of the transverse impact parameter distribution for data and simulation as a function of $1/p_{\mathrm{T}}\sqrt{\sin\theta}$ for tracks with $1 < |\eta| < 1.5$ [7].

3 Primary Vertex Reconstruction

Measured tracks are used to reconstruct the hard scatter interaction point as well as the positions of additional proton-proton collisions occurring in the same bunch crossing. The ATLAS primary vertex reconstruction [8] uses an iterative algorithm starting with a vertex finding step in which tracks are associated to a primary vertex followed by a χ^2-based vertex fit. The vertex fitter includes a beam-spot constraint.

The primary vertex resolution is extracted using data driven methods based on split vertex techniques. It is about 23 μm in the transverse plane and about 40 μm in the longitudinal plane for vertices with 70 tracks. The expected vertex reconstruction efficiency is about 95% for non-diffractive events.

4 b-tagging Algorithms and Performance

The identification of jets originating from b-quarks is an important part of the LHC physics program. Several algorithms to identify jets originating from b-quarks, referred to as b-tagging, have been developed ranging from those based on the reconstruction of an inclusive secondary vertex or the presence of tracks with large impact parameters to combined tagging algorithms making use of multi-variate discriminants. The expected performance of various b-tagging algorithms is shown in Fig. 2. The most commonly used b-tagging algorithm in ATLAS is the multi-variate algorithm MV1 which provides the best rejection of light-flavour jets for a given b-jet efficiency.

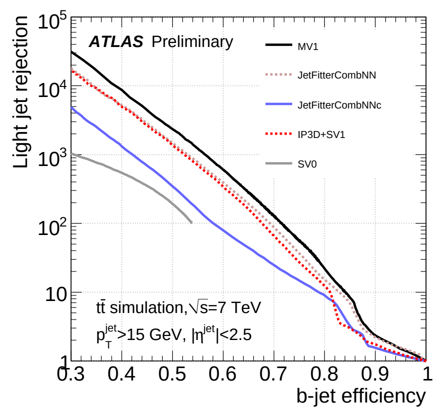

Figure 2: The rejection of light-flavour jets as a function of the b-jet efficiency for various b-tagging algorithms in a sample of simulated $t\bar{t}$ events [9].

To use b-tagging in physics analyses, the efficiency ϵ_b with which a jet originating from a b-quark is tagged by a b-tagging algorithm needs to be measured, as well as the probability of mistakenly tagging a jet originating from a c-quark or a light-flavour parton (u-, d-, s-quark or gluon g) as a b-jet, referred to as the c-tag efficiency and mistag rate respectively. Several methods have been developed to measure the b-tag efficiency, the c-tag efficiency and the mistag rate in data [9, 10, 11]. The b-tag efficiency has been measured with two methods in an inclusive sample of jets which contain muons. The c-tag efficiency has been measured in an inclusive sample of jets associated to D^* mesons while the mistag rate has been measured with two complementary methods in an inclusive jet sample. The calibration results are presented as scale factors, defined as the ratio of the efficiency (or mistag rate) in data to that in simulation. The scale factors for the MV1 algorithm at the operating point corresponding to a 70% b-tag efficiency in simulated $t\bar{t}$ events are shown in Fig. 3. For this algorithm and operating point all scale factors are consistent with unity within uncertainties.

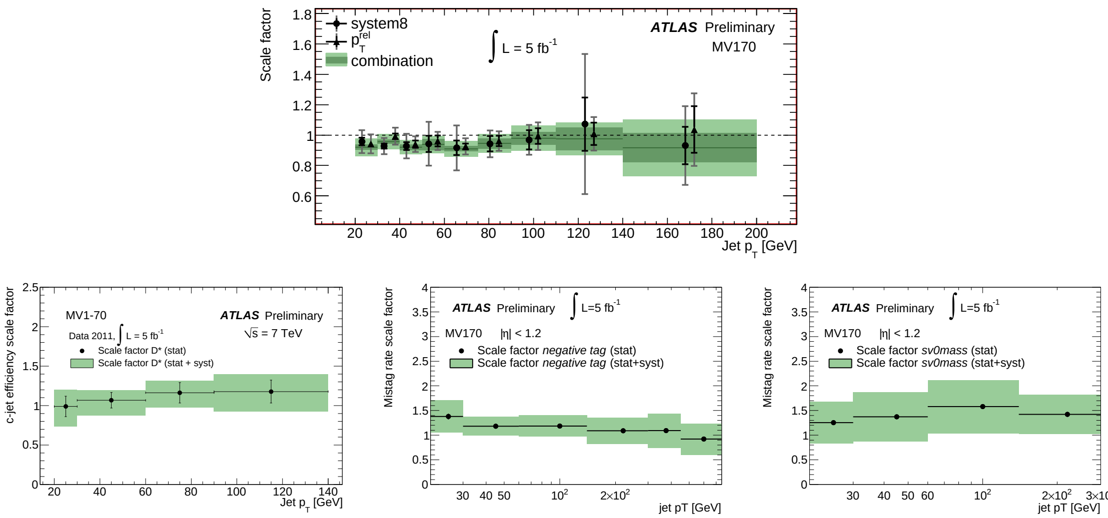

Figure 3: The data-to-simulation scale factors for the b-tag efficiency (top) [9], the c-tag efficiency (bottom left) [10] and the mistag rate (bottom middle and right) [11] as a function of p_T^{jet} for the MV1 algorithm at the operating point corresponding to a 70% b-tag efficiency in simulated $t\bar{t}$ events. The light green band in all figures indicates the total uncertainty, while the dark green band in the top figure indicates the statistical uncertainty only. In the top figure the error bars indicate both statistical and total uncertainties while the error bars in the bottom plots show statistical uncertainties only.

5 Conclusions

The ATLAS detector is designed to reconstruct tracks and vertices with high precision. A wide range of studies carried out with the 2011 data set confirm an excellent performance of the tracking, vertexing and b-tagging. This is achieved e.g. through improved alignment and track reconstruction optimized for high-pileup conditions as well as new multi-variate algorithms which have boosted the b-tagging performance.

References

[1] ATLAS Collaboration, J. Instrum. 3, S08003 (2009)

[2] L. Evans and P. Bryant, J. Instrum. 3, S08001 (2009).

[3] ATLAS Collaboration, ATLAS-CONF-2010-072, http://cdsweb.cern.ch/record/1281363.

[4] ATLAS Collaboration, CERN-PH-EP-2010-063, http://cdsweb.cern.ch/record/1309895.

[5] ATLAS Collaboration, ATLAS-CONF-2012-042, http://cdsweb.cern.ch/record/1435196.

[6] http://atlas.web.cern.ch/Atlas/GROUPS/PHYSICS/IDTRACKING/PublicPlots/ATL-COM-PHYS-2012-500/

[7] http://atlas.web.cern.ch/Atlas/GROUPS/PHYSICS/IDTRACKING/PublicPlots/ATL-COM-PHYS-2012-471/

[8] ATLAS Collaboration, ATLAS-CONF-2010-069, http://cdsweb.cern.ch/record/1281344.

[9] ATLAS Collaboration, ATLAS-CONF-2012-043, http://cdsweb.cern.ch/record/1435197.

[10] ATLAS Collaboration, ATLAS-CONF-2012-039, http://cdsweb.cern.ch/record/1435193.

[11] ATLAS Collaboration, ATLAS-CONF-2012-040, http://cdsweb.cern.ch/record/1435194.